Sol-gel synthesis of iron(III) oxyhydroxide nanostructured monoliths using Fe(NO)*9HO/CHCHOH/NHOH ternary system

Luísa Durães, Orlando Oliveira, Leandro Benedini, Benilde F.O. Costa, Ana Matos Beja, António Portugal

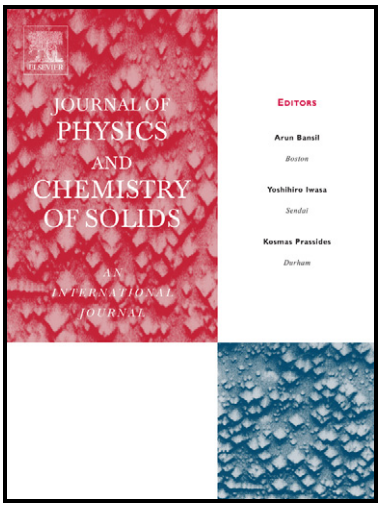

www.elsevier.com/locate/jpcs

Sol-gel synthesis of iron(III) oxyhydroxide nanostructured monoliths using $Fe(NO_3)_3 \cdot 9H_2O/CH_3CH_2OH/NH_4OH$ ternary system

Luísa Durães, Orlando Oliveira, Leandro Benedini, Benilde F.O. Costa, Ana Matos Beja, António Portugal

PII: S0022-3697(11)00053-9
DOI: doi:10.1016/j.jpcs.2011.02.020
Reference: PCS 6420

To appear in: *Journal of Physics and Chemistry of Solids*

Received date: 5 March 2010
Revised date: 11 November 2010
Accepted date: 24 February 2011

Cite this article as: Luísa Durães, Orlando Oliveira, Leandro Benedini, Benilde F.O. Costa, Ana Matos Beja and António Portugal, Sol-gel synthesis of iron(III) oxyhydroxide nanostructured monoliths using $Fe(NO_3)_3 \cdot 9H_2O/CH_3CH_2OH/NH_4OH$ ternary system, *Journal of Physics and Chemistry of Solids*, doi:10.1016/j.jpcs.2011.02.020

Sol-Gel Synthesis of Iron(III) Oxyhydroxide Nanostructured Monoliths Using $Fe(NO_3)_3 \cdot 9H_2O/CH_3CH_2OH/NH_4OH$ Ternary System

Luísa Durães[(a)*], Orlando Oliveira[(a)], Leandro Benedini[(b)], Benilde F. O. Costa[(c)], Ana Matos Beja[(c)], António Portugal[(a)]

[a] Department of Chemical Engineering, Faculty of Sciences and Technology, University of Coimbra, Pólo II, Rua Sílvio Lima, 3030-790 Coimbra, Portugal

[b] Department of Chemical Engineering, Federal University of São Carlos, Rodovia Washington Luís, km 235- SP-310, 13565-905 São Carlos, São Paulo, Brasil

[c] CEMDRX, Department of Physics, Faculty of Sciences and Technology, University of Coimbra, Rua Larga, 3004-516 Coimbra, Portugal

*Corresponding author. Tel.: +351 239798737; fax: +351 239798703. E-mail address: luisa@eq.uc.pt (L. Durães).

Abstract

Iron(III) oxyhydroxide xerogels were prepared through sol-gel technology, using iron(III) nitrate nonahydrate as precursor, ethanol as solvent and ammonium hydroxide as gelation agent. This base is used for propylene oxide substitution, which was the gelation agent in previous works. The synthesis of a gel using the NH_4OH gelation agent is an innovative result with this type of precursor, since with metal salts the addition of a strong base commonly results in precipitation of the solid. The gel synthesis was achieved by controlling the base addition time. The dried material has a residual amount of organic impurities, in contrast with the significant amount detected

in xerogels prepared using propylene oxide. The iron phase prevailing in the produced xerogels can be defined as γ-FeO(OH) (Lepidocrocite), according to FTIR and Mössbauer analyses. The xerogels are formed by large clusters of well connected nanocrystallites of this phase. XRD revealed a crystalline phase retained inside the iron oxyhydroxide amorphous structure, which corresponds to NH_4NO_3 and results from the combination of NO_3^- and NH_4^+ ions in solution. The produced xerogel has a promising composition to be an oxidizing composite for the energetic materials area.

Keywords: A. oxides, A. nanostructures, B. sol-gel growth, D. microstructure.

1. Introduction

The synthesis of metal oxides, hydroxides and oxyhydroxides through the sol-gel method is very advantageous, as it allows the formation of nanostructures with unique properties, by means of reactions that occur in a solution medium at low temperature, and only low cost laboratory equipment is required [1,2]. Other simple chemical solution processes, especially the hydrothermal approach, may also be applied to synthesize metal oxides and hydroxides nanocrystals with controlled morphologies and patterns without the use of templates (for example, nanowires and nanoplatelets) [3-6]. However the sol-gel method does not necessarily need temperatures as high as those used for hydrothermal synthesis route and also gives more versatility in the formed phases and structures in the case of iron oxides/hydroxides. Moreover, if, during the sol-gel synthesis, a certain amount of fuel is added to the metal oxide matrix, it is possible to obtain what is known as an energetic nanocomposite [7-9]. When thermally stimulated, a self-sustaining reaction is triggered, in which there is a high release of

energy. In these materials with heterogeneous condensed nature, the kinetics of the reactions is controlled by the mass transfer rate of the reactants. Thus, their nanostructured nature allows an improved reactivity, which results from their small size and high surface area. If, in these nanocomposites, the fuel is a metal, a thermite system is obtained [8,10,11].

Thermite systems can be used as energetic materials for pyrotechnic compositions (switches; delay mixtures; igniters; *etc.*) and as additives to increase the performance of propellants and explosives. Other applications include torches for underwater or atmospheric cutting and perforation, hardware destruction devices, gas generators for airbags, the production of alumina-iron liners *in-situ* for pipes, and portable heat sources [10]. On the other hand, the iron(III) oxides, by themselves, are important materials in various fields of application [12]. They are used as inorganic pigments, both natural and synthetic, and as efficient catalysts for the manufacture of styrene, the Fisher-Tropsch synthesis of hydrocarbons, the selective oxidation of polyaromatic hydrocarbons and the burning of fuels, among other reactions. They are the starting material for the production of ferrites (*e.g.* $SrBaFe_{12}O_{19}$ and $Fe_{12}O_{19}$) and can also be used to produce ceramic components, digital storage devices, permanent magnets, semiconductor layers, abrasive and polishing agents and gas sensors. Moreover, in nanometer size, they also have application in new electronic and optical devices, magnetic recording media, magnetic coolers, magnetic resonance imaging and bioprocessing ferrofluid technology.

The sol-gel process is a synthesis process that takes place at temperatures below 100 ºC, in the liquid phase, and using either salts or metal alkoxides as precursors. The produced solids are mostly oxides, hydroxides and oxyhydroxides resulting from inorganic polymerization chemistry. This involves the hydrolysis of the precursor and

the subsequent formation of M-O-M and M-OH-M (M - metal) bridges by condensation reactions, producing a colloidal suspension named sol; with further condensation, the suspension gives rise to a gel, which has the solvent and the catalyst trapped inside the nanostructured oxide/hydroxide network [2, 13-15]. When the liquid phase is removed, a solid nanoporous material with oxide properties is produced [16]. There are different ways to remove the liquid from the gel structure: i) removal by evaporative drying at ambient pressure or in vacuum, with resulting structures known as xerogels; ii) removal through the use of supercritical conditions, in which structures known as aerogels are formed [13]. The former are less porous and, therefore, denser than the aerogels. The reason for this is the evaporation process. In fact, for the case of xerogels, the shrinkage of the pores occurs, through the action of pressure gradients generated by the effect of surface tension at the solid-liquid-gas interface. In supercritical drying conditions these tensions are not present [17,18]. Thus, the aerogels are highly porous materials, as the three-dimensional solid structure of the gel is maintained almost intact.

The sol-gel technology allows a microstructural control of the final product, resulting in compounds with tailored and uniform characteristics (composition, density, particle size and morphology). In the case of thermite energetic nanocomposites, it is clearly important that the oxide structure is correctly formed, as the energetic reactions of these compounds depend on the reactants particle size, as well as of the surface area and porosity of their structure. The intimate contact between the compounds is essential because it reduces the diffusion distances between the fuel and the metal oxide.

In this work, an iron oxide was synthesized by sol-gel technology, which can be used as a basis for thermite energetic nanocomposites synthesis. For the iron oxide formation, an iron nitrate nonahydrate salt was used as precursor. Its dissolution in a solvent,

usually ethanol, in the presence of a few equivalents of water, allows the hydrolysis of the Fe(III) hexa-aquo ion, at low pH. The result is a hydroxo-aquo ion precursor with the structure $[(Fe(OH)(OH)_2)_5]^{2+}$ [2,15,19]. The hydrolysis reaction can be induced by the addition of a proton acceptor, that is, with a compound that acts as a base. After the initial hydrolysis, it follows a condensation mechanism of the olation type (hydroxo bridges), with formation of the structures $[(H_2O)_5Fe(OH)Fe(OH_2)_5]^{5+}$ and $[(H_2O)_4 Fe(OH)_2Fe(OH_2)_4]^{4+}$, and of the oxolation type as well, with the formation of the structure $[(H_2O)_5FeOFe(OH_2)_5]^{4+}$ [2,15,19]. The represented ions are responsible for the jelly-like look of the oligomers that result from the condensation, by the same mechanisms, of colloidal particles of the sol. Thus, a three-dimensional solid network is formed – gelation process. In this structure, the proportion of hydroxo and oxo bridges cannot be estimated and, therefore, the product should be designated as iron oxide/hydroxide [19,20].

Propylene oxide can be used as proton acceptor, since it acts as a weak base, receiving the H^+ released in the formation of the $[(Fe(OH)(OH)_2)_5]^{2+}$ cation and increasing their formation and also the pH of the medium. Once protonated, the propylene oxide undergoes a ring opening reaction by the influence of nucleophilic agents, such as water and the nitrate ion. The reaction with nitrate generates 2-nitrooxy-2-propanol, whereas the reaction with water originates 1,2-propanediol. The reaction with water should be avoided, since it regenerates H^+ ions, inhibiting the formation of the hydroxo-aquo cation, necessary for the gel formation. For this reason, the equivalents of water in the solution must be scarce, with the only purpose of hydrating the Fe^{3+} ion [19-21]. However, propylene oxide is a toxic compound, very volatile and carcinogenic, that leads to the formation of branched alcohols (more complex), difficult to remove during

the drying process. The organic impurities that are trapped inside the xerogel significantly decrease the energetic performance of the nanocomposites that can be produced with this material [11,18]. It is therefore interesting to study alternative proton acceptors for the propylene oxide replacement. A possible option is the use of ammonium hydroxide that is often applied in sol-gel chemistry to obtain silica gels. The ammonium hydroxide reacts with the H^+ ions from the Fe(III) hydrolysis and generates H_2O molecules, as well as the NH_4^+ ion. It is possible that the later bonds to the free NO_3^- ion in solution, forming the NH_4NO_3 salt.

Thus, this work presents an experimental procedure where the ammonium hydroxide was used to replace propylene oxide, leading to the formation of an iron oxide/hydroxide gel. It should be emphasized that the formation of a gel by the use of this gelation agent is an innovation, since it is more common that this type of base leads to the formation of precipitates when the precursors are metal salts. In this study, only evaporative drying was used, thus only xerogels were produced.

The formed products were characterized by: Elemental Analysis, to determine the mass percentages of the chemical elements in the samples, thus assessing the amount of organics existent in the xerogel; Fourier Transform Infrared Spectroscopy (FTIR), to identify the functional groups in the structure of the xerogel; X-Ray Diffraction (XRD), to identify crystalline phases; Mössbauer Spectroscopy, for the determination of solid phases with iron; Scanning Electron Microscopy (SEM), for the observation of the microstructure and topography of the particles/clusters; Nitrogen Gas Adsorption, to determine the specific surface area and the pore size distribution of the material.

2. Experimental

2.1 Gel synthesis

In a typical synthesis, 5.2 g of $Fe(NO_3)_3.9H_2O$ were dissolved in 5 cm^3 of ethanol, under permanent magnetic stirring at 200-300 rpm. The temperature of the solution was maintained at 60 °C, using a glass jacket fed by a thermostatic water bath. After dilution, the solution was orange colour. In a second step, 5.6 cm^3 of an ammonium hydroxide solution (10 M) were added, drop by drop, during about 15 minutes, in order to promote a gradual pH rise. During this time, the pH evolution and the temperature of the solution were measured with a *pH 213 – Microprocesser pH Meter*, from *Hanna Instruments*. After adding the total volume of the base, a dark brown gel was formed.

2.2 Gel drying (xerogel formation)

The evaporative drying of the gel consisted of two stages. First, the sample was kept for two days inside a ventilated oven, at 60 ^oC, to remove most of the liquid retained in the gel. After this, the sample was kept for three days inside a vacuum oven, at 70 ^oC and 10^{-5} bar, to finish the removal of impurities. At the end, the obtained xerogel exhibited dark brown colour (near black) and small fissures.

2.3 Xerogel characterization

The xerogel was prepared for physical and chemical characterization. For this, it was milled in a ball mill *Crescente Dental*, model *Wig-L-Bug*. Four xerogel batches, with the same synthesis and drying conditions, were mixed and taken for characterization. The only technique in which the material was analyzed as obtained after drying was the scanning electron microscopy.

2.3.1 Chemical characterization

Elemental Analysis: The mass percentages of C, H, N, S and O in the sample were measured, in order to quantify the amount of impurities trapped in the xerogel. An *EA 1108 CHNS-O* equipment was used, from *Fisons Instruments*. For C, H, N and S determination, the sample combustion was undertaken in the equipment oven at 900 ^{o}C, and using a stream of He enriched with oxygen. The equipment separates and quantifies the gases from this combustion, using a chromatographic column and a thermal conductivity detector, respectively. To determine the oxygen, the sample pyrolysis was done with the oven at 1060 ° C. The generated gases were separated by a chromatographic column and quantified with a thermoelectric detector.

Fourier Transform Infrared Spectroscopy: With this technique, the main functional groups inside the xerogel structure may be identified. Small amounts of the sample were taken for analysis and were mixed with KBr in a mass ratio of 1:10. The resulting mixture was pressed in a mould and pellets were obtained for the analysis in a *Nicolet 6700 FTIR* spectrometer, from *ThermoScientific.* The used range of wave numbers was 400-4000 cm^{-1}, with a spectral resolution of 4 cm^{-1} and 64 scans per sample. *OMNIC* software allowed the analysis control and the results processing.

X-Ray Diffraction: This technique was used to identify the crystalline phases present in the material, including the expected ammonium nitrate phase. A powder diffractometer was used, with a *Enraf Nonius FR590 (3 kW)* generator with a quartz *Jhoanssen* monochromator, coupled to a Curved Position Sensitive detector *INEL CPS 120* for data

acquisition, and a processing system which included the database *PC-PDF*, from *JCPDS-ICDD*, and the *Search-Match* program *UPDSM*. For the analysis, the milled sample was introduced into a capillary with 0.3 mm diameter, rotating about its axis with constant speed. The sample analysis in the capillary occurs in transmission geometry, and the data acquisition time time was 24 h. The equipment operates with a Cu X-ray source (linear focus) and the applied voltage and current were, respectively, 42 kV and 40 mA.

Mössbauer spectroscopy: The resulting spectrum from this technique allows the identification and quantification through parameters of the electrical, magnetic and mixed interactions between the ^{57}Fe nuclei and their electrons, thus making possible to quantify the iron phases in the sample. The equipment used was a Mössbauer spectrometer with transmission geometry, using the 14 keV γ radiation from a source of ^{57}Co/Rh with a strength of about 25 mCi, a modulator of radiation energy by movement in a triangular speed wave and constant acceleration, and a radiation proportional detector. The spectrum was obtained at room temperature and its adjustment to a set of Lorentzian lines was carried out by least squares. The reference absorbent was a sheet of metallic iron (α-Fe), with 25 μm thickness.

2.3.2 Physical characterization

Scanning electron microscopy: This technique allowed the observation of size, morphology and appearance of particles/clusters of the material and the topography of its surface. To improve the images resolution, which would be conditioned by the fact that the sample had low electrical conductivity, an Au film was deposited on the sample

surface, using the PVD technique (Physical Vapour Deposition). The deposition time was 30 s. After the metallization, the sample was analyzed in a *JEOL JMS-5310* scanning electron microscope.

Nitrogen gas adsorption: This technique was used to determine the specific surface area, pore size distribution, pore surface area and pore volume of the material. Before the analysis, the sample was degassed at 200 ^{o}C in vacuum (10^{-5} bar) during 24 h, to remove adsorbed species. In the analysis, volumes of the adsorbed nitrogen at five different relative pressures (0.05 to 0.2) were taken at 77 K, to obtain the specific surface area by the BET theory. The desorption isotherm and the BJH theory were used for the porosimetry measurements.

3. Results and discussion

As mentioned before, four replicates of the synthesis and drying procedures were performed, being the xerogel average weight of ~ 4 g per synthesis. It was necessary to increase the bath temperature for the synthesis from 25 ^{o}C to 60 ^{o}C, relatively to the procedure previously used with propylene oxide [11,18,21]. Only with this change, favorable energy conditions were met for the gel formation with the utilization of the ammonium hydroxide gelation agent.

3.1 pH results

Figure 1 shows the pH and temperature evolution in the system during the time of the gel formation.

Until near 300 s there is a gradual pH increase, which is due to the base addition and consequent neutralization of the H^+ ions that are formed by the hydrolysis reaction. This increase is accompanied by an increase of the solution temperature, which demonstrates that condensation reactions are also occurring. From 300 s, when parts of the dark brown solution already show a gelatinous structure, the pH and temperature tend to remain approximately constant, but the pH still growing residually. After 900 s, with the addition of the entire base volume, gel becomes cohesive.

3.2 Chemical characterization of the xerogel

3.2.1 Elemental analysis

The results of elemental analysis are shown in Table 1. The wt.% errors associated with the measurements are ±0.43, ±0.20, ±0.25 and ±0.15, for C, H, N and O, respectively. The second sample of the table corresponds to a white salt crystallized on the walls of the beaker after the drying end. The values of elemental analysis obtained for this salt are close to the values calculated for ammonium nitrate compound (wt.% N = 35.1; wt.% O = 59.9; wt.% H = 5.0). Still, it was detected some amount of impurities with carbon.

Table 2 presents some theoretical values obtained for comparison with the experimental results of Table 1, and based on two scenarios for the xerogel composition: Fe_2O_3, NH_4NO_3, and NH_4^+ (Hypothesis 1) or FeO(OH), NH_4NO_3 and NH_4^+ (Hypothesis 2). The preceding scenarios represent, in the case of Hypothesis 1, the exclusive existence of oxo bridges in the iron phase (in other words, a situation of complete condensation) and, in the case of Hypothesis 2, the coexistence of oxo and hydroxo bridges in equal

proportion. In both cases, it was considered that other substances or impurities have completely evaporated.

Comparing the xerogel values in Table 1 with the values in Table 2, it is concluded that both the hypothetic compositions of the final product are possible, but the presence of ammonium nitrate is also confirmed by these results. The large amount of N present (resulting from NH_4NO_3 and NH_4^+) does not allow drawing conclusions about the iron phase of the xerogel. Experimentally (Table 1), a residual amount of impurities with carbon was also detected, possibly organics resulting from the interaction of ethanol with nitrated substances. These impurities are present, however, in a much lower amount than that reported in previous work with propylene oxide gelation agent [18], where the wt.% C in the xerogel was approximately 17 %. Thus, the synthesis procedure presented here leads to significantly better results than the process with propylene oxide in what concerns the removal of the organic impurities.

3.2.2 Fourier transform infrared spectroscopy (FTIR)

In Figure 2 are presented the results of FTIR analysis of the xerogel.

In the range between 400 and 800 cm^{-1}, it's possible to observe three broad peaks (minimums at 466, 606 and 694 cm^{-1}– peaks a, b and c), which can be attributed to Fe-O bonds in oxides and oxyhydroxides, as evidenced by the bibliographic revision in [11]. Their overlapping and width and the amorphous nature of the material may contribute to differences in their minimum points regarding the expected from the literature. The intense absorption observed at 825 cm^{-1} (peak d) may be due to the bending vibrations of –OH…O groups in the oxyhydroxides [11,22], but can also be ascribed to the contribution of NH_3 groups from the ammonia salts (800-1200 cm^{-1})

[23], if the minimum intensity point of this absorption (~ 900 cm^{-1}) is slightly shifted in the case of the sample of this work.

It is also possible to note broad and less intense peaks in the range 1000-1150 cm^{-1} (minimums at 1011, 1037 and 1127 cm^{-1} – peaks e, f and g), which can be attributed to stretching vibrations of C-O in primary alcohols (1010-1050 cm^{-1}), due to the remaining ethanol, or eventually secondary alcohols (1100-1150 cm^{-1}), by the combination of ethanol with nitrated species [22].

Between 1200 and 1700 cm^{-1} a very intense and broad absorption appears (minimum at 1423 cm^{-1} – peak h), followed by a weaker absorption, between 1500 and 1650 cm^{-1} (minimum at 1626 cm^{-1} – peak i), which may be due to the stretching vibrations of the -NO_2 group in the ammonium nitrate salt (1240-1350 cm^{-1}; 1515-1560 cm^{-1}) and the bending vibrations of the -NH_3^+ group of the same salt (1500 cm^{-1}; 1600-1775 cm^{-1}) [22]. These peaks may yet have the contribution of the bending vibrations of the C-H bonds in CH_3 and CH_2 groups (1370-1470 cm^{-1}) [22] of the residual alcohol and of -OH bonds from the iron phase and adsorbed water (1615-1630 cm^{-1}; detected by the slight characteristic oscillation in the curve) [22,23]. The well-defined peak with minimum at 1763 cm^{-1} (peak j) can also be justified by the absorption of -NH_3^+ group of the ammonium nitrate salt, according to the characteristic band at 1600-1775 cm^{-1} already referred [23].

The small double peak close to 2100 cm^{-1} and the peaks that appear between 2300 and 2450 cm^{-1} (minimums at 2304, 2348, 2396 and 2426 cm^{-1}) – regions k, l and m – are characteristic from CO_2 absorption [23], which is due to the contamination of the analysis environment.

At the range of 2750 to 3000 cm^{-1}(region n) it is possible to observe slight changes in the curve that can be ascribed to the stretching vibrations of C-H bonds in the -CH_2 groups (2850-2925 cm^{-1}) and CH_3 groups (2870-2960 cm^{-1}) of the residual alcohol [22]. The broad absorption between 3000 and 3600 cm^{-1} (broad peak o) is mainly due to the stretching vibrations of the NH_3^+ group (3150-3350 cm^{-1}) and the –N-H bonds (3100-3500 cm^{-1} (linked); 3350-3550 cm^{-1} (not linked)), by the presence of ammonium nitrate, and the stretching vibrations of the –O-H bonds linked by hydrogen bonds in the iron phase [22,23]. It may still have a slight contribution of the –O-H bonds of adsorbed water and residual alcohol. The slight oscillation observed between 3600 and 3900 cm^{-1} (region p) is also due to the stretching vibrations of the –O-H bonds, but not linked [22,23].

This analysis confirms that the obtained xerogel retains a residual amount of organic compounds (alcohol and its derivatives) in its structure and an appreciable amount of ammonium nitrate salt. It also follows that the iron phase of the xerogel has Fe-O bonds and some OH groups.

3.2.3 X-ray diffraction

Figure 3 shows the X-ray diffractogram obtained for the xerogel. The observed diffraction pattern fits well on the pattern of the NH_4NO_3 phase indexed with the number 08-0452 in the PC-PDF database from ICDD. The crystallographic planes that originate the main diffraction peaks are indicated in the figure, but all the minor peaks that appear on the right also belong to this phase. The referred ammonium nitrate phase has an orthorhombic crystalline system with lattice parameters a = 4.952 Å, b = 5.438 Å and c = 5.745 Å. The match level obtained was 86 %, with a merit figure equal to 148.

The phases that followed on the adjustment list had a merit figure of only 49 or less and presented no chemical coherence regarding the studied system. This result allows proving the existence of NH_4NO_3 in the xerogel. It also leads to the conclusion that the constituent iron phase of the xerogel is amorphous, certainly due to the nanometric size of its crystallites.

3.2.4 Mössbauer spectroscopy

Figure 4 presents the Mössbauer spectrum obtained from the xerogel analysis at room temperature. The solid line represents the fit of Lorentzian curves to experimental points and it is moved up from these points to obtain a better visualization. The obtained doublet is characteristic of paramagnetic phases, which do not exhibit a hyperfine magnetic field – H (in Tesla). Table 3 presents the obtained parameters for this doublet. The found isomer shift is characteristic of the phase γ-FeO(OH) (Lepidocrocite) [24,25], in which the oxidation state of iron is 3+ and Fe atoms are in octahedral sites surrounded by six O and O-H. The obtained QS value is not equal to the indicated in the literature for this phase (QS = 0,55(1) mm/s), being however very near. Anyway, the QS also depends on the material grain size and, therefore, is less representative than the IS for phases identification. The paramagnetic nature of the synthesized xerogel agrees with the literature data for the γ-FeO(OH) phase.

3.3 Physical characterization of the xerogel

3.3.1 Scanning electron microscopy

In Figure 5 are shown xerogel images obtained by scanning electron microscopy with two different magnifications. To obtain these images, the working distance was 22 mm

and the electrons accelerating voltage was 10 kV. A low voltage was used because small explosions were observed on the material surface by the effect of the energy of the electron beams generated with higher voltages. This chemical instability may be related to the bursting of the NH_4NO_3 crystals due to the heating caused by the electron beam.

Figure 5 (left) shows that the iron phase is present in agglomerated form. The smooth appearance of the cluster surface leads to the conclusion that the material is formed by agglomeration of nanometer-sized crystallites, in accordance with the observed with similar materials in a previous work [21]. When using the x5000 magnification (Figure 5 (right)) it is possible to note incrustations on the material surface, which are resultant from the presence of the NH_4NO_3 crystals dispersed on the iron phase.

3.3.2 Nitrogen gas adsorption

In figure 6 are shown the graphic results obtained from xerogel analysis by nitrogen gas adsorption. The obtained adsorption isotherm (Figure 6 (A)) is of Type II, since the amount adsorbed tends to infinity when P/P_0 tends to unity, which corresponds to the adsorption of overlapped multiple layers. It is not possible to observe the phenomenon known as hysteresis that is usually associated with the expansion of less rigid porous structures and the irreversible adsorption of molecules with size close to the pore width. Figure 6 (B) evinces that the material has pores in the ranges of mesopores and micropores.

With the used technique, the BET theory was applied to obtain the specific surface area, and the BJH theory (desorption) was used to obtain porosimetry indicators - Table 4.

By comparing the values in Table 6 with those obtained in previous work with the propylene oxide as gelation agent [11,18], it happens that the material here synthesized has specific surface area, pore specific surface area and pore specific volume very much lower (about 20 fold) when compared with the xerogels obtained with the propylene oxide, what can be due to the presence of the NH_4NO_3 salt. It is also concluded that the xerogel is predominantly a mesoporous material.

4. Conclusions

The aim of this study was to produce iron oxide/hydroxide gels, based on the precursor $Fe(NO_3)_3.9H_2O$ and replacing the gelation agent used in previous work (propylene oxide) by the ammonium hydroxide. This objective was achieved, since, for the first time, gels were obtained starting from the ternary system $Fe(NO_3)_3{\cdot}9H_2O$ / CH_3CH_2OH / NH_4OH.

From the synthesized material characterization, it was concluded that the removal of the alcohol was more efficient in xerogels produced from the ammonium hydroxide. In these, there was the presence of a crystalline phase, identified by XRD as ammonium nitrate, being this salt dispersed inside the amorphous iron phase. By Mössbauer spectroscopy it was concluded that γ-FeO(OH) (Lepidrococite) was the constituent phase of the obtained xerogel. It was also found that the material had a mesoporous structure and was composed of clusters of nano-sized crystallites. Its specific surface area proved to be much smaller than the one obtained for xerogels where propylene oxide was used as gelation agent.

In future studies, xerogel filtration/washing processes will be implemented, in order to remove the amount of ammonium nitrate dispersed into it. However, it is also possible

to note advantages from the salt presence inside the gel structure. Thus, the xerogel produced may have potential application as an oxidizing mixture in the energetic materials area, namely in thermite systems. It combines the metal oxide/hydroxide and an oxidizing very common in energetic materials, ammonium nitrate, which by the reason of being less stable than the first one, may favour the ignition conditions of the thermite charges produced when a fuel is added to the xerogel.

5. Acknowledgments

The authors gratefully acknowledge to Arménio Serra for the experimental support on the FTIR analysis and Chymiotechnon for the FTIR facility.

6. References

1. C.J. Brinker and G.W. Scherer, Sol-Gel Science – The Physics and Chemistry of Sol-Gel Processing, Academic Press, Boston, 1990, Ch. 2.

2. J. Livage, M. Henry and C. Sanchez, Sol-gel chemistry of transition metal oxides, Prog. Solid State Chem. 18 (1988), 259-341.

3. M. Yoshimura, Powder-less processing of nano-ceramics: How we can realize their direct fabrication from solutions and/or melts, in: J.-F. Baumard (Ed), Lessons in Nanotechnology – From Traditional and Advanced Ceramics, Techna Group, Faenza, 2005, p. 161.

4. 5. G. Zou, H. Li, Y. Zhang, K. Xiong and Y. Qian, Solvothermal/hydrothermal route to semiconductor nanowires, Nanotechnology 17 (2006), S313-S320.

5. G. Zou, K. Xiong, C. Jiang, H. Li, T. Li, J. Du and Y. Qian, Fe_3O_4 Nanocrystals with Novel Fractal, J. Phys. Chem. B 109 (2005) 18356-18360.

6. G. Zou, H. Li, D. Zhang, K. Xiong, C. Dong and Y. Qian, Well-Aligned Arrays of CuO Nanoplatelets, J. Phys. Chem. B 110 (2009) 1632-1637.

7. A.E. Gash, R.L. Simpson, T.M. Tillotson, J.H. Satcher Jr. and L.W. Hrubesh, Making nanostructured pyrotechnics in a beaker, in: Int. Pyrotech. Semin. USA (Ed), Proc. 27th Int. Pyrotech. Semin., IIT Research Institute, Chicago, 2000, p. 41.

8. T.M. Tillotson, A.E. Gash, R.L. Simpson, L.W. Hrubesh, J.H. Satcher Jr. and J.F. Poco, Nanostructured energetic materials using sol-gel methodologies, J. Non-Cryst. Solids 285 (2001), 338-345.

9. T.M. Tillotson, R.L. Simpson, L.W. Hrubesh and A. Gash, Method for Producing Nanostructured Metal-Oxides, United States Patent No. US 2002/0104599 A1.

10. S.L. Fischer and M.C. Grubelich, Theoretical energy release of thermites, intermetallics, and combustible metals, in: Int. Pyrotech. Semin. USA (Ed), Proc. 24th Int. Pyrotech. Semin., IIT Research Institute, Chicago,1998. p. 231.

11. L. Durães, Study of the Reaction Between Iron(III) Oxide and Aluminum and Evaluation of Its Energetic Potential, PhD Thesis, Faculty of Sciences and Technology of University of Coimbra, Coimbra, 2007, Chs. 2, 4.

12. R. Zboril, M. Mashlan and D. Petridis, Iron(III) oxides from thermal processes-synthesis, structural and magnetic properties, Mössbauer spectroscopy characterization, and applications, Chem. Mater. 14 (2002), 969-982.

13. A.C. Pierre and G. Pajonk, Chemistry of aerogels and their applications, Chem. Rev. 102 (2002), 4243-4265.

14. R.M. Cornell and U. Schwertmann, The Iron Oxides: Structure, Properties, Reactions, Occurrences and Uses, Wiley-VCH, Weinheim, 2003, Ch. 13.

15. J.-P. Jolivet, M. Henry and J. Livage, Metal Oxides Chemistry and Synthesis: From Solution to Solid State, John Wiley & Sons, Chichester, 2000, Part I.

16. M.B. Bhusham, Synthesis of Ordered Nanoenergetic Composites, MSc Thesis, Faculty of Graduate School of University of Missouri-Columbia, Columbia, 2005.

17. M.A. McHugh and V.J. Krukonis, Supercritical Fluid Extraction, 2nd Ed., Butterworth-Heinemann, Boston, 1994.

18. A.L. Santos, Study of the Formation of an Iron Oxide Aerogel with Supercritical Fluid Drying, Chemical Engineering Graduation report, Faculty of Sciences and Technology of University of Coimbra, Coimbra, 2006, Ch. 3.

19. A.E. Gash, T. M. Tillotson, J.H. Satcher Jr., J.F. Poco, L.W. Hrubesh and R.L. Simpson, Use of epoxides in the sol-gel synthesis of porous Iron(III) oxide monoliths from Fe(III) salts, Chem. Mater. 13 (2001), 999-1007.

20. A.E. Gash, R.L. Simpsom and J.H. Satcher, Strong akaganeite aerogel monoliths using epoxides: synthesis and characterization, Chem. Mater. 15 (2003), 3268-3275.

21. L. Durães, B.F.O. Costa, J. Vasques, J. Campos and A. Portugal, Phase investigation of as-prepared iron oxide/hydroxide produced by sol–gel synthesis, Mater. Lett. 59 (2005), 859-863.

22. H.G.O. Becker, W. Berger, G. Domschke, E. Fanghänel, J. Faust, M. Fischer, F. Gentz, K. Gewald, R. Gluch, R. Mayer, K. Müller, D. Pavel, H. Schmidt, K. Schollberg, K. Schwetlick, E. Seiler and G. Zeppenfeld, Organikum, 2nd Ed., Fundação Calouste Gulbenkian, Lisboa, 1997, Ch. 3.

23. L.-E. Amand and C.J. Tullin, The Theory Behind FTIR analysis – Application Examples From Measurement at the 12 MW Circulating Fluidized Bed Boiler at Chalmers, CECOST, Lund University, Sweden, 1999.

24. N.N. Greenwood and T.C. Gibb, Mössbauer Spectroscopy, Chapman and Hall, New York, 1971.

25. C. McCammon, Mössbauer spectroscopy of minerals, in: T.J. Ahrens (Ed), Mineral Physics and Crystallography - A Handbook of Physical Constants, American Geophysical Union, Washington, 1995, p. 332.

Figure Captions:

Figure 1 – pH and temperature variation during the synthesis of the gel. The starting time corresponds to the addition of the first ammonium hydroxide drop.

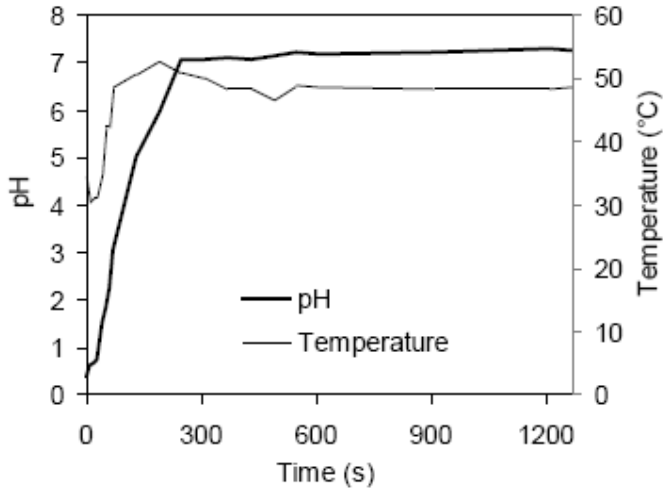

Figure 2 – FTIR spectrum of the xerogel.

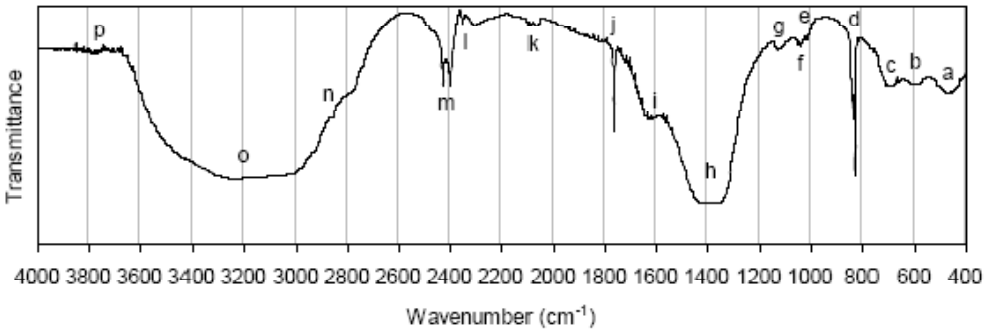

Figure 3 – X-ray diffractogram of the xerogel.

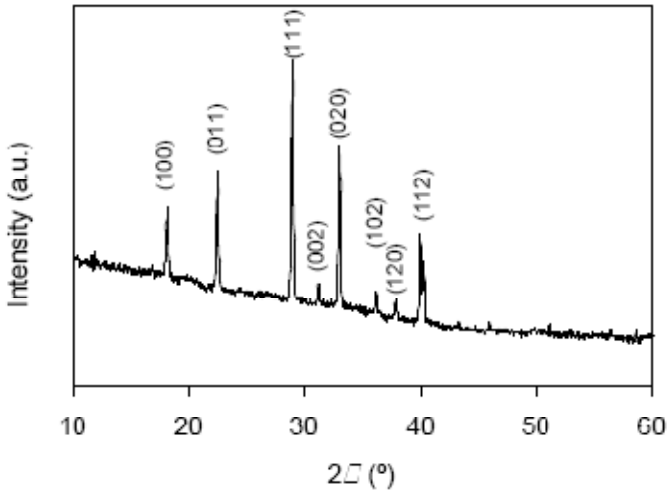

Figure 4 – ^{57}Fe Mössbauer spectrum of the xerogel, taken at room temperature.

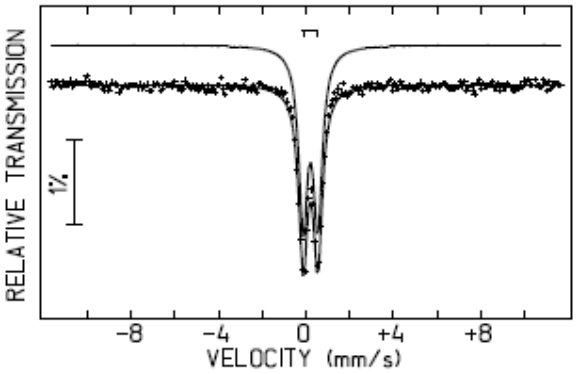

Figure 5 – Xerogel images obtained by scanning electron microscopy with two magnifications: x500 (on the left) and x5000 (on the right).

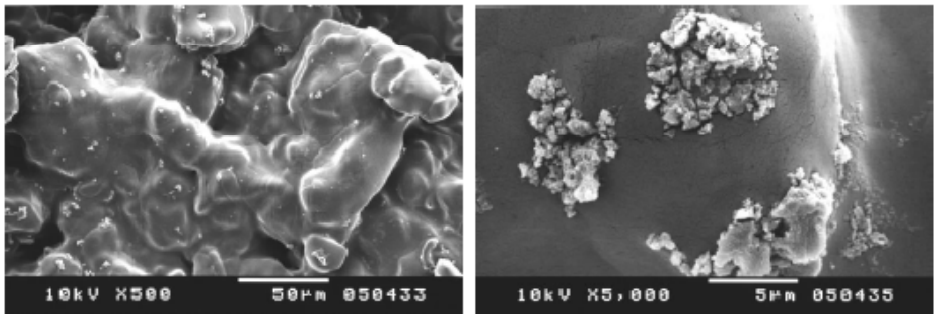

(left) (right)

Figure 6 – Results of the xerogel analysis by nitrogen gas adsorption: (A) adsorption-desorption isotherms and (B) pore volume as function of their size.

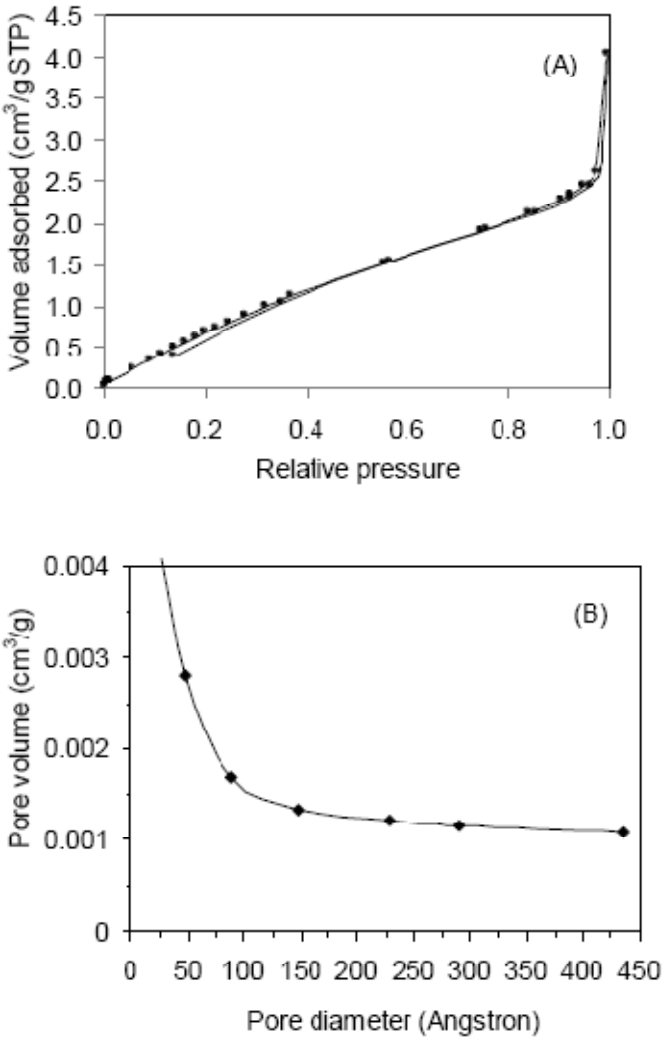

Table 1 – Elemental analysis results.

Sample	wt.% C	wt.% H	wt.% N	wt.% O
Xerogel	0.20	4.96	25.20	48.81
Salt	2.54	6.27	36.56	51.53

Table 2 – Estimated values for elemental mass percent in the xerogel.

Hypothesis	wt.% C	wt.% H	wt.% N	wt.% O
1[(a)]	-	5.1	30	49
2[(b)]	-	5.2	29	50

(a) Products: Fe_2O_3, NH_4NO_3, NH_4^+; (b) Products: FeO(OH), NH_4NO_3, NH_4^+.

Table 3 – Mössbauer parameters for the xerogel sample.

Isomer Shift (IS) (mm/s)	Quadrupole Splitting (QS) (mm/s)	Line Width (mm/s)
0.30(1)	0.68(1)	0.49(1)

Table 4 – Surface area and porosimetry indicators obtained for the xerogel.

Surf. Area (BET) (m^2/g)	Pore Surf. Area (BJH) (m^2/g)	Pore Vol.(BJH) (m^3/g)	Mean Pore Diam.(BJH) Å
4.15 ± 0.12	2.39	0.002996	50.21

Research highlights for manuscript PCS-D-10-00208R1

> γ-FeO(OH) xerogels were produced using iron(III) nitrate nonahydrate precursor. > Monolithic gels were never obtained with this precursor and NH_4OH gelation agent. > Large clusters of well connected nanocrystallites of iron oxyhydroxide. > NH_4NO_3 by-product is retained inside the iron oxyhydroxide structure. > Promising oxidizing composite for the energetic materials area.